

Mechanical Properties of Bonded Elastomer Discs Subjected to Triaxial Stress

P. A. KAKAVAS*

Department of Chemical Engineering, University of Southern California, Los Angeles, California 90089

SYNOPSIS

The aim of this article was to evaluate and analyze the mechanical properties of bonded elastomer discs subjected to triaxial stress on an MTS (machine for testing samples) equipment. Several pulling tests were run on an Instron machine using an O-ring type of samples to evaluate the mechanical properties of testing unfilled nitrile rubber subjected to uniaxial tension. It was found from the stress-strain curve of the O-ring samples that a very small stress softening occurred when the maximum strain is less than 200%. It was also found that the stress and strain at break does not drastically vary with respect to strain rate. The initial modulus does not vary with respect to strain rate up to $\dot{\epsilon} = 2 \text{ min}^{-1}$, and only for large values of $\dot{\epsilon}$ does the modulus depend on the strain rate. The material used for the uniaxial tension experiments were bonded between two rigid cylindrical steel plates and the specimens were subjected to uniaxial tension on an MTS machine. It was found that the initial modulus in tension was smaller than in compression. The theoretical predicted initial modulus from Gent's equation was much larger than experimentally estimated. It was shown that the elastomer in the pancake tests was not incompressible and a value of 0.494 was determined for the effective Poisson's ratio. A mathematical equation was derived for the effective Poisson's ratio as a function of the volume fraction of voids within the testing material. © 1996 John Wiley & Sons, Inc.

INTRODUCTION

Rubberlike materials are well known for their low shear modulus and their capability of sustaining large recoverable deformations. However, it is not well known as to their poor resistance to cavitation when they are subjected to a triaxial state of stress. Because of its importance to the understanding of the microfracture process, reinforcement, adhesive, joint strength, and explosive decompression, several years ago, we started investigating the microcavitation process in thin elastomer discs with its top and bottom surfaces pokerchip glued to rigid plates. Following the previous researchers,^{1,2} they call this type of specimen a pokerchip; however, in this article, it will be called a *pancake*. This type of specimen was chosen because with an appropriate aspect

ratio of diameter to thickness a state of stress close to a negative pressure field can be conveniently generated at the center of the specimen when it is subjected to simple uniaxial tension.³⁻⁷

It was found in our early studies⁸⁻¹² that the first detectable microcavitation as monitored with an *acoustic emission* sensor happened at about 40% of the yield strain and microcavitation results in significant mechanical softening of the specimen.^{8,10,11} The softening was attributed to the increase of void content due to continuous microcavitations. The apparent initial stiffness of the specimen is a function of the aspect ratio and can be theoretically estimated.² However, in the process of our study, we found that, depending on the molding conditions and mold design, the apparent stiffness of some specimens deviated from the theoretical value and relatively fewer acoustic emission events at small strains were observed from these specimens. This article presents experimental facts as well as a theoretical explanation of this abnormal behavior.

* Present address: 31 Kanakari Street, 262 23 Patras, Greece.

EXPERIMENTAL

The chemical composition of the material used for this study is given in Table I. All the ingredients described in Table I were well mixed in an open two-roll mill, and to estimate the curing time of the compound, a *cure-curve* was obtained from the cone Rheometer.¹³ Figure 1 shows the curemeter curve for the testing materials which indicates a minimal curing time 4.5 min.

O-ring type of samples were cut from the milled batch of rubber and they were placed in an O-ring mold. Samples were cured in a press machine at $T_c = 370^\circ\text{F}$, $P_c = 640$ psi, and $t_c = 4.5$ min. After the completion of the curing process, the mold was removed from the press machine and the samples were taken out from the mold. Before the O-rings specimens were subjected to uniaxial tension in an Instron machine, they were left at atmospheric conditions for several hours.

An Instron tensile testing machine was used for tensile tests. O-rings were held between the spools of pneumatic grips and they were stretched at a constant speed from 0.1 to 20 in./min. The initial modulus was determined by stretching O-ring specimens at very low speed (0.1 in./min), and a high chart speed was maintained to increase the accuracy of strain determination. The initial modulus was then calculated from the slope of the stress-strain curve at zero strain. A more accurate determination of the initial modulus can be performed by plotting the ratio stress/strain (σ/ϵ) vs. the strain (ϵ) at low speed.

Uniaxial mechanical properties of the vulcanizates was measured using a number of O-ring specimens. The inside diameter of the O-rings was 1.859 in. and their thickness was 0.1270 in. (within less than 1% error). A micrometer was used for measuring the thickness of each sample. The O-rings were tested on an Instron testing machine for a variety of crosshead speeds from 0.1 to 20 in./min.

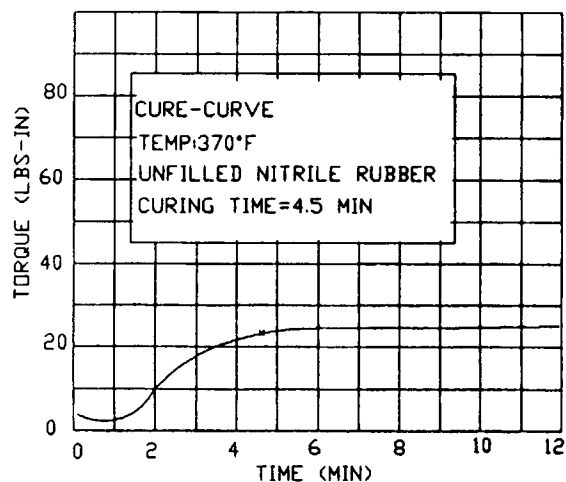


Figure 1 Curemeter curve from an unfilled nitrile rubber.

A number of pancake specimens were also prepared for mechanical tests for the study of the microcavitation process within these types of specimens. Thin cylindrical pieces cut from the mixed batch were sandwiched between two metal plates and placed in an appropriate mold for curing. The metal surfaces were first sandblasted and well cleaned by a suitable solvent. A primer coat (Chemlock 205) was sprayed on the surface of the metal plates and they were left overnight to dry at room temperature. The bonding agent (Chemlock 250) was sprayed on the top of the Chemlock 205 and was dried for several hours. The inside of the mold was sprayed with a silicon mold release to ease the removal of the bonded rubber cylinder. All the samples were cured at $T_c = 370^\circ\text{F}$, $P_c = 1600$ psi, and $t_c = 45$ min and the long curing time was selected to give sufficient time for the temperature in the elastomer disc to reach 370°F . The diameter of all samples was 6 in. and the thickness was varied from 0.2 to 0.4 in., i.e., the aspect ratio (D/h) (varies from 30 to 15). The pancake specimens were tested on

Table I Chemical Composition of the Unfilled Nitrile Rubber Samples

Chemical Compound	Parts (g)	Density (g/cc)	Vol. Fraction v_i
NBR (Krynac-800)	100.0	1.060	.949821
Zinc oxide	5.0	5.470	.009203
Stearic acid	1.0	0.847	.011887
<i>N</i> -Isopropyl- <i>N</i> -phenyl- <i>p</i> -phenylenediamine	1.0	1.300	.007745
Magnesium carbonate-treated elemental sulfur	2.0	2.070	.009728
Benzothiazyl disulfide	1.5	1.300	.011617
Total	110.5		

an MTS (machine for testing samples), and to examine the possible fracture mechanisms within the deformed specimens, the so-called *acoustic emission* (AE) was applied. The results of this nondestructive method from the pancakes were presented in previous articles.^{8,10} To examine the possible volume change in the pancake specimen, the lateral contraction was measured at the midplane of the specimen using a caliper.^{9,11,12}

Along the course of these studies, samples (pancake) of the geometry shown below were tested. These samples were subjected to uniaxial tension or *triaxial stress* on an MTS machine. The pulling speed of the piston was kept constant ($u_p = 0.01$ in./min) for all the tests. The strain rate $\dot{\epsilon}$ was also kept constant for every test, but it depends on the thickness of the specimen. In our experiments, the $\dot{\epsilon}$ was varied between 0.0265/min and 0.0488/min. In other words, the experiments on the bonded elastomer disks were conducted at a low strain rate.

RESULTS AND DISCUSSION

Stress Response of Unfilled O-ring Nitrile Rubber Samples

The inside and the outside diameters of the testing O-ring (sample B-2) was $d_i = 1.895$ in. and $d_o = 1.996$ in., respectively. The cross-section area A_0 of the sample was 0.0685 in.² The O-ring was placed between two spools on the Instron testing machine. When no load was applied on the O-ring, the separation distance between the spools was equal to $d_0 = 1.803$ in. [see eq. (A-1)] and the radius of each spool was equal to $c = 0.25$ in.

Figure 2 shows the response of an O-ring rubber sample subjected to uniaxial tension. The sample was pulled up to 100% strain and it was left to return to undeformed state with the same speed as in the loading case ($\dot{\epsilon} = 0.352$ in.⁻¹).

Small hystereses were observed along the unloading path of the samples. After the first run was over, the O-ring was subjected to 220% strain and it was left to return again to the undeformed state. On the third run, the sample was pulled to rupture.

Figure 2 indicates that the engineering stress and strain at break are $\sigma_b = 250$ psi and $\epsilon_b = 400\%$, respectively. The strain computation was based on eq. (A-8). The stress computations were based on the undeformed area A_0 of the O-ring, and it is usually called *nominal stress*.¹ To calculate the initial modulus of the material, a plot of the nominal stress divided by the strain (σ/ϵ) vs. strain (ϵ) was made

(see Fig. 2). The intersection of the straight line with the vertical axis at zero strain indicates the initial modulus of the material, whose value is equal to $E = 216$ psi.

The pronounced hysteresis observed in the first stress cycle of unfilled rubber (Fig. 2) manifests irreversible processes. The next constant strain rate cycles are then always nearly reproduced, showing, in general, a weak hysteresis mainly originated with relaxation. A phenomenological treatment of this effect was given by Mullins and Tobin.¹⁴⁻¹⁶

Variation of the Initial Modulus and Stress and Strain at Break with the Strain Rate

Several unfilled nitrile rubber O-rings were tested with a variety of strain rates.¹¹ The chemical composition of the testing O-ring specimens is depicted in Table I. Table II shows the average values of the initial modulus E and the stress σ_b and strain ϵ_b at break for various values of strain rate $\dot{\epsilon}$. Figure 3 shows the variation of $\langle E \rangle$ vs. the strain rate $\dot{\epsilon}$. Clearly, it can be seen from the graph that the average modulus $\langle E \rangle$ remains constant up to strain rate $\dot{\epsilon} = 2$ min⁻¹, and after that, the $\langle E \rangle$ value increases rapidly as the strain rate increases.

Since the average modulus does not change with respect to the variation of strain rate (for low values of $\dot{\epsilon}$), this indicates that the material does not exhibit *viscoelasticity* at low $\dot{\epsilon}$. However, at large $\dot{\epsilon}$, the viscoelasticity starts playing an important role and we attribute the hysteresis in the stress/strain curve (Fig. 2) to the existence of voids within the O-rings.

A plot of the average value of stress σ_b and strain ϵ_b at break as a function of strain rate $\dot{\epsilon}$ is shown in Figure 4. We observe that both curves do not show a significant increase with respect to strain rate. This indicates that the viscoelasticity is not a primary factor in the uniaxial extension of an unfilled nitrile rubber. In Figure 4, we observe that the strain at break ϵ_b oscillates around the average value $\langle \epsilon_b \rangle = 3.51$ in./in.

A plot of stress at break σ_b vs. the strain at ϵ_b is shown in Figure 5. All the points fall on a straight line of slope $\gamma = 1.56$. This graph is usually called the Smith's plot.^{17,18}

The Reduced Mooney-Rivlin Representation

A discussion of the stress-strain behavior of unfilled systems in terms of a reduced mechanical equation of state provide some interesting and novel insights: The reduced mechanical equation of state in the mode of simple tension, is given by¹⁸:

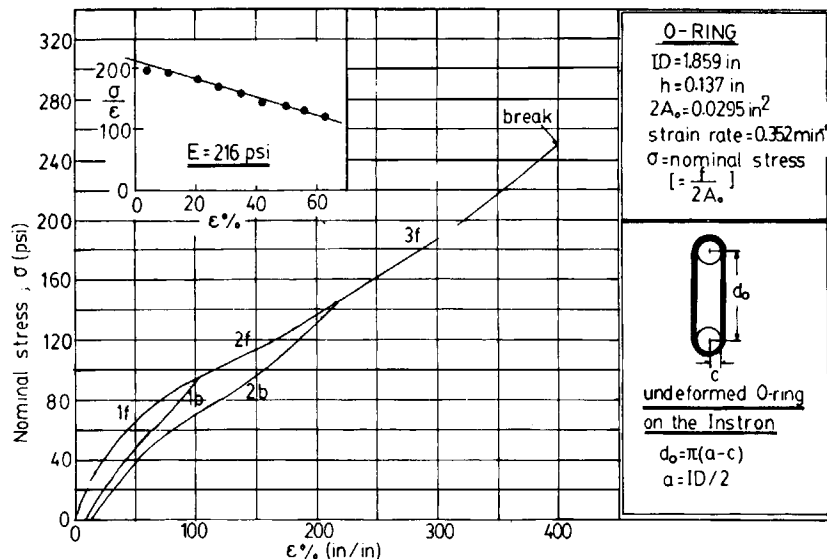


Figure 2 Observed stress–strain curve with hysteresis from an unfilled nitrile rubber subjected to uniaxial tension.

$$\frac{\sigma}{\left(\lambda - \frac{1}{\lambda^2}\right)} = 2C_1 + 2 \frac{C_2}{\lambda} \quad (1)$$

where σ denotes the Piola stress (nominal stress), and λ , the principle extension and C_1 and C_2 represent the Mooney–Rivlin constants.¹⁹

A plot of $\sigma/(\lambda - \lambda^{-2})$ vs. the inverse of the principle extension ($1/\lambda$) is shown in Figure 6. All the points up to 150% strain fall on a straight line of slope $2C_1 = 42$ psi and interection $2C_2 = 32$ psi with respect to vertical axis at $1/\lambda = 0.0$. The intersection of the same line with the axis $1/\lambda = 1$ represents the shear modulus G of the unfilled nitrile rubber whose chemical composition is given in Table I. The shear modulus of the material was found being equal to $G = 72$ psi and the Young’s modulus E is equal to $3G$, i.e., 216 psi, which is equal to the value es-

timated from the plot σ/ϵ vs. ϵ of Figure 2. A modification of the reduced mechanical equation of state for simple tension of filled systems was derived by Kilian and Schenk.²⁰

Fitting the Experimental Data

Blatz–Kakavas Equation

Several mathematical equations have been proposed for fitting the stress–strain curve of an unfilled rubber.¹⁹ In this article, we propose the following equation for fitting the experimental curve:

$$e = \left(1 + a \frac{t}{E}\right)^{1/a} - 1 \quad (2)$$

where $e = \ln(\lambda)$ represents the logarithmic strain (λ being the extension ratio), a is a parameter to

Table II Average Value of the Stiffness E and Nominal Stress and Strain at Break for Various Values of Strain Rate

U_p (in./min)	ϵ (min^{-1})	$\langle E \rangle_{\text{psi}}$	$\langle \sigma_b \rangle_{\text{psi}}$	$\langle \epsilon_b \rangle$ (in./in.)
20	7.052	260.5	299.0	3.79
10	3.526	233.0	306.0	4.63
5	1.763	189.0	272.0	4.46
1	0.3526	187.75	202	3.63
0.2	0.0705	183.66	152	2.64
0.1	0.03526	184.02	224	3.67

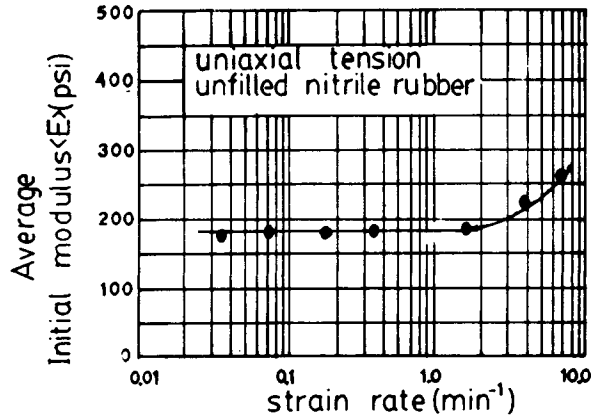


Figure 3 Initial modulus vs. strain rate from an unfilled nitrile rubber subjected to uniaxial tension.

be determined by fitting, E indicates the modulus of the material, and t denotes the Cauchy stress.

Figure 7 shows the experimental points with solid dots from an unfilled nitrile rubber whose chemical composition is given in Table I. Equation (2) fits the experimental points up to $e = 1.2$ or equivalently up to strain $\epsilon = 232\%$. In other words, the proposed equation is doing very well for small and moderate high strains. Equation (2) cannot fit well the points near the rupture of the material.

One-term Ogden's Equation

For simple tension, the one-term Ogden's equation is given by¹⁹:

$$t = \frac{2G}{\eta} (\lambda^\eta - \lambda^{-\eta/2}) \tag{3}$$

where G represents the shear modulus ($G = E/3$); η is an undetermined parameter, to be determined by fitting the eq. (3) with the experimental data; and t denotes the Cauchy stress based on the deformed cross-section area of the O-ring.

In terms of the logarithmic strain e , eq. (3) can be readily rewritten as follows:

$$t = \frac{2G}{\eta} \left[\exp(\eta e) - \exp\left(-\frac{\eta}{2} e\right) \right] \tag{4}$$

Taking $\eta = 1.6$, eq. (4) fits very well all the experimental points up to break (see Fig. 7).

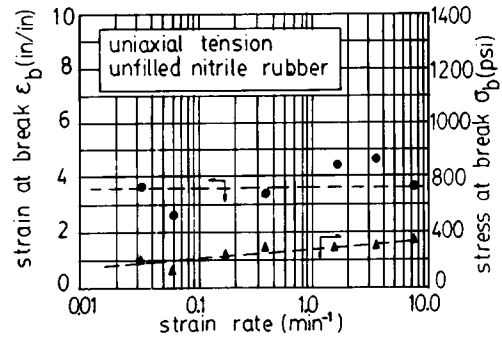


Figure 4 Nominal stress and strain at break vs. strain rate from an unfilled nitrile rubber.

STRESS-STRAIN BEHAVIOR OF BONDED ELASTOMER DISCS SUBJECTED TO TRIAXIAL STATE OF STRESS

Figure 8 shows the geometry of the testing pancake samples. Figure 9 shows a typical observed stress-strain curve at low strain values from the triaxial stress test (pancake) of the unfilled nitrile rubber whose chemical composition is described at Table I.

For all the testing specimens, the modulus in tension varied from 6100 to 2700–2500 psi, whereas the modulus in compression varied from 4400 to 6100 psi. When the material was tested in tension for the second time, the modulus was reduced approximately 8–10%. In contrast, the modulus in compression remains almost the same as in the first run. The modulus in each case was estimated by taking the slope along the straight part of the curves as shown in Figure 9. The slack at the beginning of the deformation does not allow one to estimate precisely the modulus in tension and compression. However, the modulus in tension is *smaller* than in compression ($M_C/M_T \approx 2.259$).

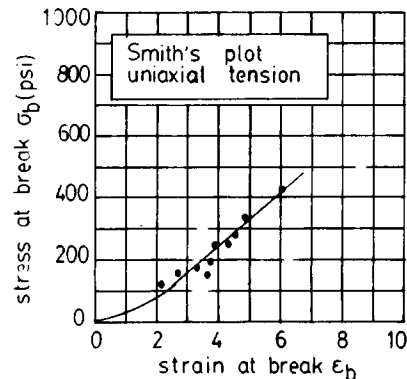


Figure 5 Stress at break σ_b vs. strain at break ϵ_b (in./in.).

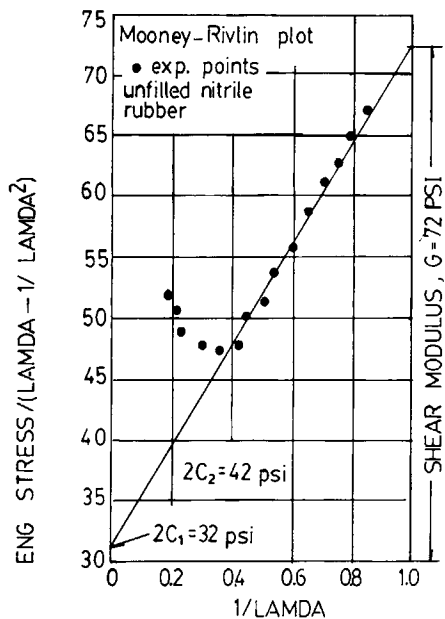


Figure 6 Unfilled nitrile rubber stress-strain curve in terms of the reduced variables.

The lateral contraction as a function of the strain ϵ was given in Ref. 11. All the points at low strain fall on a straight line whose slope is about 0.378. All the other points fall on a straight line whose slope is 0.234. If we denote by $-u_0(a)/a$ the lateral contraction at the middle plane of the sample, then the equation of the lateral contraction vs. strain, at low strain, is given by

$$-\frac{u_0(a)}{a \cdot \epsilon} = 0.378 \quad (5)$$

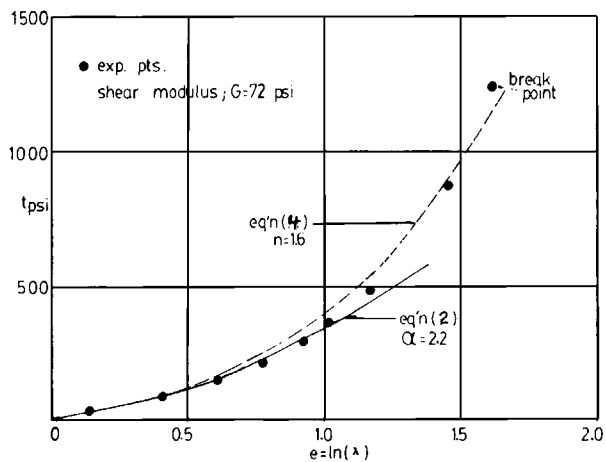


Figure 7 Fitting the uniaxial data with one term in Ogden's strain energy function and with Blatz-Kakavas equation.

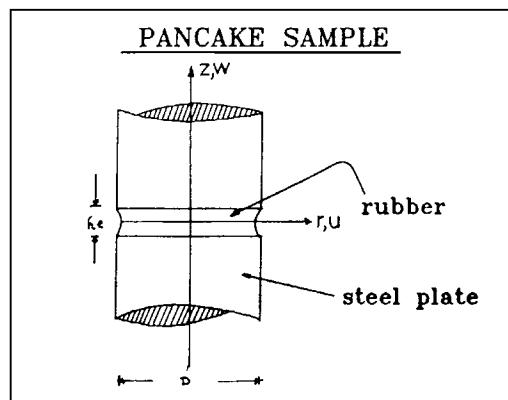


Figure 8 Typical geometry of a pancake sample.

where a is the radius of the sample. As will be discussed in the next section, eq. (1) suggests that the elastomer disk is not truly incompressible.

According to Gent's equation^{4,5} for incompressible solids, the modulus of the pancake M , with respect to the Young's modulus, is given by

$$\frac{M}{E} = 1 + 2S^2 \quad (6a)$$

where the geometric factor S is defined by

$$S = \frac{D}{4h} \quad (6b)$$

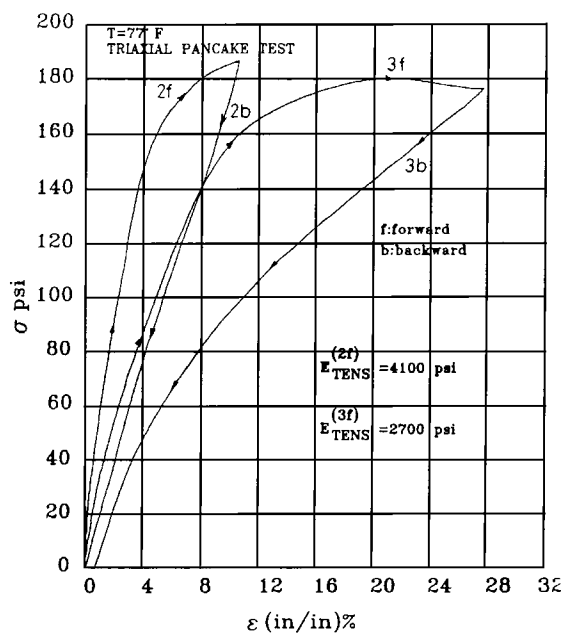


Figure 9 Process stress-strain curve at low strain from the triaxial test experiment in tension and compression.

Table III The Lateral Contraction over Strain δ , as a Function of the Poisson's Ratio ν

ν	0.450	0.460	0.470	0.475	0.477	0.478	0.480	0.485	0.490	0.493	0.495	0.499
δ	0.141	0.161	0.188	0.208	0.217	0.222	0.233	0.267	0.322	0.373	0.424	0.634

and D and h define the diameter and the thickness of the pancake, respectively. Since, the Young's modulus for this material is 180 psi (see Fig. 2) and the geometric factor S is about 7.5, the modulus of the pancake should be theoretically equal to 20,429 psi. Obviously, this value is much higher than that observed from our experimental measurements (see Fig. 9). Equations (6) also predict that the modulus in compression and tension must be equal. In contrast, our experimental observations show that there is a difference between these two moduli.

The questions that we must pose at this point are the following:

- (i) Why is $M_{\text{calc}} \gg M_{\text{obser}}$?
- (ii) Why is the modulus in tension and compression different?
- (iii) What is the reason for the stress softening along the successive loading of the specimen? In this article, we will give a complete answer to the first question and speculative accounts will be taken for answers to the second and the third questions.

EFFECTS OF VOIDS ON THE RESPONSE OF UNFILLED BONDED NITRILE ELASTOMER DISCS SUBJECTED TO TRIAXIAL STRESS

The geometry of a testing sample and the coordinate system used for the analysis is shown in Figure 8. Let us denote by a and h the radius and the thickness of the specimen, respectively. Following the *linear stress analysis*, it can be shown^{8,11,12} that the displacement fields $u(r, z)$ and $w(z)$ are

$$u, (\rho, z) = Al_1(\rho)[1 - 4z^2/h^2] \quad (7a)$$

$$w(z) = w(z) \quad (7b)$$

where $\rho = kr$, $\kappa = 2/h[(3 - 6\nu)/(2 - 2\nu)]^{1/2}$, $I_1(\rho)$ defines the *modified Bessel function of first order*, and the coefficient A is given by

$$A = \frac{-1.5\varepsilon\nu a}{(1 - \nu)kaI_0(ka) - (1 - 2\nu)I_1(ka)} \quad (8)$$

where $I_0(\cdot)$ and I_1 define the *modified Bessel functions of zero and first order*, respectively, and ε defines the strain within the pancake specimen. Substitution of eq. (8) into (7) yields the *lateral contraction* at the middle plane of the pancake ($z = 0$, $r = a$) i.e.:

$$\frac{-u_0(a)}{a} = \frac{1.5\nu\varepsilon}{(1 - \nu)m - (1 - 2\nu)} \quad (9)$$

where

$$m = ka \frac{I_0(ka)}{I_1(ka)}; \quad \left(ka = a^* \sqrt{\frac{6(1 - 2\nu)}{(1 - \nu)}} \right) \quad (10)$$

When $a \rightarrow 0$, then $m \rightarrow 2$ and eq. (5) becomes²¹

$$\frac{-u_0(a)}{a} \rightarrow \frac{3\nu\varepsilon}{2} \quad (11)$$

When $a \rightarrow \infty$, then $m \rightarrow ka$ and eq. (5) becomes²¹

$$\begin{aligned} & -\frac{u_0(a)}{a} \\ &= \frac{3\nu\varepsilon}{2\{a^*[6(1 - 2\nu)(1 - \nu)]^{1/2} - (1 - 2\nu)\}} \quad (12) \end{aligned}$$

where $a^* = a/h$ (a = radius, h = thickness). A typical value of a^* for our experiment was about $a^* = 8$. At $a^* = 8$, m is close to ka ; using eq. (9) for the lateral contraction and (12), the value of the effective Poisson's ratio ν_{eff} , may easily be determined. Using either the tables or IMSL subroutines for the estimation of the $I_0(ka)$ and $I_1(ka)$, one obtains the following values (see Table III) of the diametral contraction $\delta = u_0(a)/a\varepsilon$ as a function of ν .

As Table III indicates for $\delta = 0.378$, the effective Poisson's ratio must be equal:

$$\nu_{\text{eff}} = 0.494 \quad (13)$$

This low value of the Poisson's ratio indicates that the elastomer disc in the pancake is not incompressible ($\nu = 0.5$). Also, we know that a homogeneous unfilled nitrile rubber is incompressible. *Why does such an apparent contradiction exist?* We attri-

bute this to the existence of *voids* in the pancake, whose appearance possibly was introduced during molding. It can be shown^{9,12} that the volume dilatation is given by

$$\frac{\Delta V}{V_0} = \epsilon \frac{(1 - \nu)m - 1}{m(1 - \nu) - (1 - 2\nu)} \quad (14)$$

where V_0 defines the initial value of the material, i.e., $V_0 = \pi a^2 h$ and $\Delta V = V - V_0$ (V = final volume of the sample). When $a \rightarrow 0$, then eq. (10) becomes

$$\frac{\Delta V}{V_0} = \epsilon(1 - 2\nu) \quad (15)$$

When $a \rightarrow \infty$, then eq. (10) becomes

$$\frac{\Delta V}{V_0} = \epsilon \frac{a^*(6(1 - 2\nu)(1 - \nu))^{1/2} - 1}{a^*(6(1 - 2\nu)(1 - \nu))^{1/2} - (1 - 2\nu)} \quad (16)$$

For $\nu = 0.494$, eq. (12) yields

$$\frac{\Delta V}{V_0} = 0.7024 \quad (17)$$

i.e., the volume dilatation increases linearly with respect to apparent strain ϵ of the pancake.

ESTIMATION OF INITIAL VOIDS CONTENT

Following Warren's idea,²² we assume that all the voids in an incompressible material are located in a sphere of initial radius A , and the rest of the rubber is molded in a spherical shell of initial radius B , of the same center as that of the sphere A . Since the material is *incompressible*, we may write¹⁹

$$\frac{du}{dr} + 2\frac{u}{r} = 0 \quad (18)$$

The solution of this simple equation is

$$u(r) = \frac{B_0}{2} \quad (19)$$

and the radial and tangential Piola stresses are¹⁹

$$\sigma_r = -p - \frac{4GB_0}{r^3} \quad (20)$$

$$\sigma_\theta = -p + \frac{2GB_0}{r^3} \quad (21)$$

Substitution of (18) and (19) into the equilibrium equation, i.e.,

$$r \frac{\partial \sigma_r}{\partial r} + 2(\sigma_r - \sigma_\theta) = 0 \quad (22)$$

yields $p = \text{constant} = p_0$. The boundary conditions

$$\sigma_r = 0 \quad \text{at} \quad r = a; \quad \sigma_r = T \quad \text{at} \quad r = b \quad (23)$$

yield the value of B_0 , i.e.:

$$B_0 = \frac{Tb^3a}{4G(1 - a)} \quad (24)$$

where $a = (A/B)^3$ and the value of p_0 , i.e.:

$$p_0 = -\frac{T}{1 - a} \quad (25)$$

From the stress-strain curve of the pancake sample (see Fig. 9), we observe that the apparent yield point occurs at $\epsilon \approx 10\%$, at which the volume dilatation is 0.07024 .

It can readily be shown^{9,12} that the modulus M of the pancake may be related to the Young's modulus E of the material via the following equation:

$$\frac{M}{E} = \frac{1}{(1 - 2\nu)(1 + \nu)} \times \left[(1 - \nu) - \frac{2\nu^2}{(1 - \nu)m - (1 - 2\nu)} \right] \quad (26)$$

When $a \rightarrow 0$, then $m \rightarrow 2$ and eq. (14) yields $(M/E) \approx 1$. When $a \rightarrow \infty$, then $m \rightarrow ka$ and (26) yields

$$\frac{M}{E} = \frac{1}{(1 - 2\nu)(1 + \nu)} \left[(1 - \nu) - \frac{2\nu^2}{a^*(6(1 - 2\nu)(1 - \nu))^{1/2} - (1 - 2\nu)} \right] \quad (27)$$

Equation (27) yields the ratio M/E as a function of the aspect ratio a^* and the Poisson's ratio ν . Letting $a^* = 8$, then using either the tables or the IMSL subroutines ratio, M/E can be obtained for different values of ν . Table IV shows the ratio M/E vs. ν .

Table IV The Modulus of the Pancake Normalized upon the Young's Modulus as a Function of the Poisson's Ratio; Aspect Ratio = 8.0

ν	0.470	0.475	0.480	0.485	0.490	0.492	0.493	0.494
M/E	4.66	5.33	6.26	7.67	10.06	11.56	12.52	15.07

Our experiments have shown that the ratio M/E is of order of 15 (Fig. 9, curve 2f). Note that the measurements for the lateral contraction were taken during the loading path 2f. Hence, from Table IV, the Poisson's ratio is about 0.494, which agrees with the measured value from the lateral contraction measurements.

Substitution of (22) and (25) into (20) and (21) yields the stresses σ_r and σ_θ , i.e.,

$$\sigma_r = \frac{T}{1-a} \left[1 - \frac{b^3 a}{r^3} \right] \quad \text{and} \quad \sigma_\theta = \left[1 + \frac{b^3 a}{2r^3} \right] \frac{T}{1-a} \quad (28)$$

Substitution of (24) into (19) yields the displacement $u(r)$. Indeed,

$$u(r) = \frac{Tb^3 a}{4G(1-a)r^2} \quad (29)$$

Assume now that the material is *compressible without holes*; then, the stresses σ_r and σ_θ are defined in spherical coordinates by²³

$$\sigma_r = \frac{2G}{1-2\nu} [(1-\nu)u_r + 2\nu u/r] \quad (30a)$$

$$\sigma_\theta = \frac{2G}{1-2\nu} [\nu u_r + u/r] \quad (30b)$$

where $u_r = du/dr$.

The displacement field $u(r)$ must satisfy the equilibrium eqs. (22) and the boundary conditions, i.e.:

$$u(r=0) = 0 \quad \text{and} \quad u(r=b) = u_b \quad (30c)$$

Substitution of eqs. (30a) and (30b) and utilizing the boundary conditions (30c), the displacement $u(r)$ at any point in the compressible sphere is

$$u(r) = \frac{u_b}{b} r \quad (30d)$$

Since $\sigma_r = T$ is on the outer surface of the sphere, eq. (30) yields the hydrostatic tension T on the outer surface, i.e.:

$$T = \frac{2(1+\nu)G}{1-2\nu} \frac{u_b}{b} \quad (31)$$

Evaluating (29) at $r=b$ and equating $u(b)/b$ to u_b/b via eq. (31), one obtains the relation between a and ν . Indeed,

$$\nu_{\text{eff}} = \frac{2-3a}{4-3a} \quad (32)$$

Substitution of eq. (32) into (12) yields the *lateral contraction* as a function of a , i.e.:

$$-\frac{u_0(a)}{a\varepsilon} = \frac{0.5(2-3\alpha)}{2\alpha^*(\alpha)^{1/2} - \alpha} \quad (33)$$

So, experimentally, it was found that the left-hand side of (33) is equal to 0.234; eq. (33) yields that the volume fraction of voids is $a = 0.0978$.

Replacing ν by its equivalent expression (32) into eq. (27), one obtains the modulus of the pancake as a function of a . Indeed,

$$\frac{M}{E} = \frac{4-3a}{9a(1-a)} \left[1 - \frac{\{2-3a\}^2}{2m-3a} \right] \quad (34)$$

where

$$m = ka \frac{1_0(ka)}{1_1(ka)} \quad ka = 3a^* a^{1/2} \quad (35)$$

Equation (34) correlates the modulus of the pancake sample with the Young's modulus of the material and the volume fraction of the voids ($a^* = a/h$ [aspect ratio]).

CONCLUSIONS

During this research investigation, it was found that the unfilled nitrile rubber O-ring sample subjected

to uniaxial tension does not exhibit viscoelastic effects for low strain rates. However, they do show viscoelastic behavior whenever the O-ring is pulled at high strain rates. It was also shown that the one-term Ogden strain energy function fits the uniaxial data very well, whereas the Mooney–Rivlin function of two parameters does not fit the experimental data for large extensions. Experimental stress–strain curves were also extracted from the pancake type of samples subjected to uniaxial tension. It was shown that the modulus of elasticity is very low compared to theoretical computations through Gent’s equation. The softening of the material was attributed to the existence of voids within the prepared pancake samples. Following linear stress analysis, the modulus of elasticity for the pancake tests was computed as a function of Poisson’s ratio and the aspect ratio a . From the experimental evaluation of the ratio M/E , one can easily compute the Poisson’s ratio for the testing material. It was found that for the testing material $\nu = 0.494$. Following Warren’s approach, one can also find the connection between the Poisson’s ratio and the void content a , and we found that for our testing material $a = 9.78\%$.

APPENDIX A

Strain Computation in an O-ring Rubber Sample

When an O-ring sample is subjected to tension in an Instron machine, it is placed between two spools of radius c (see Fig. 2). The initial distance d_0 , between the spools can be readily found using the equation

$$d_0 = \pi(\alpha - c) \quad (\text{A.1})$$

where a denotes the inner radius of the O-ring. The initial volume of the O-ring sample is given by

$$V_0 = h_0\pi(b^2 - a^2) \quad (\text{A.2})$$

where b denotes the outer radius of the sample.

When the O-ring is stretched, then the volume of the sample becomes

$$V = h \int_0^e [2d + 2\pi(c + x)] dx \quad (\text{A.3})$$

where

$$h = \frac{h_0}{\sqrt{\lambda}} \quad \text{and} \quad e = \frac{b - a}{\sqrt{\lambda}}$$

Integration of eq. (A.3) yields

$$V = 2(d + c) \frac{b - a}{\sqrt{\lambda}} + \pi \frac{(b - a)^2}{\lambda} \frac{h_0}{\sqrt{\lambda}} \quad (\text{A.4})$$

where $d = d_0 + \Delta d$, d_0 is given by eq. (A.1) and Δd denotes the displacement of the O-ring from the unstretched state.

Assuming that the O-ring elastomer specimen is *incompressible*, then the left-hand side of eqs. (A-2) and (A-4) are equal. Hence,

$$\omega^3 - 2A\omega - B = 0 \quad (\text{A.5})$$

where

$$\omega^2 = \lambda \quad (\text{A.6})$$

and

$$A = \frac{\frac{d}{\pi} + c}{b + a}, \quad B = \frac{b - a}{b + a} \quad (\text{A.7})$$

The solution of the (third degree) algebraic eq. (A.5) is given by

$$\lambda = \omega^2 \left[\left(\frac{B^2}{4} + \Delta \right) + B\sqrt{\Delta} \right]^{1/3} + \left[\left(\frac{B^2}{4} + \Delta \right) - B\sqrt{\Delta} \right]^{1/3} + 2 \left(\frac{B^2}{4} + \Delta \right)^{1/3} \quad (\text{A.8})$$

where

$$\Delta = \frac{1}{(b + a)^2} \left[\left(\frac{b - a}{2} \right)^2 - \frac{B}{27} \frac{\left(\frac{d}{\pi} + c \right)^3}{(b + a)} \right] \quad (\text{A.9})$$

Therefore, given Δd , we calculate $d = d_0 + \Delta d$ and then we estimate the extension ratio λ via eq. (A.8).

The author is indebted to Drs. P. J. Blatz and W. V. Chang for helpful discussions on this experimental research and also for teaching him the theory of rubber elasticity. Most of the work was carried out at the Department of Chemical Engineering, University of Southern California, Los Angeles, CA 90089, and at Parker Hannifin Corp., Culver City, Los Angeles, CA 90230.

REFERENCES

1. G. H. Lindsey, R. Schapery, M. Williams and A. Zak, Aerospace Research Laboratories Report ARM, 63-152, September 1963.
2. M. Williams and R. Schapery, *Int. J. Fract. Mech.*, **1**, 64 (1965).
3. B. Wijayatha, W. V. Chang, and R. Salovey, *Rubb. Chem. Technol.*, **51**, 1006 (1978).
4. A. Gent and P. Lindley, *Proc. R. Soc. Lond. A*, **249**, 195 (1945).
5. A. Gent and D. Tomplins, *J. Appl. Phys.*, **40**(6), 2520 (1969).
6. R. Denecour and A. Gent, *J. Polym. Sci. Part A-2*, **6**, 1853 (1968).
7. A. Gent and D. Tomplins, *J. Polym. Sci. Part A-2*, **7**, 1483 (1968).
8. P. Kakavas and W. V. Chang, *J. Appl. Polym. Sci.*, **42**, 1997 (1991).
9. P. Kakavas and P. J. Blatz, *J. Appl. Polym. Sci.*, **43**, 1081 (1991).
10. P. Kakavas and W. V. Chang, *J. Appl. Polym. Sci.*, **45**, 865 (1992).
11. P. Kakavas, PhD Dissertation, University of Southern California, 1987.
12. P. J. Blatz and P. A. Kakavas, *J. Appl. Polym. Sci.*, **49**, 2197 (1993).
13. R. O. Babbit, Ed., *Rubber Handbook*, R. T. Vanderbilt Co., 30 Winfield Street, Norwalk, CT 06855, 1978.
14. L. Mullins and N. R. Tobin, *Rubb. Chem. Technol.*, **30**, 355 (1957).
15. L. Mullins and N. R. Tobin, *J. Appl. Polym. Sci.*, **9**, 2993 (1965).
16. L. Mullins, *Rubb. Chem. Technol.*, **42**, 339 (1969).
17. T. L. Smith, *J. Polym. Sci. A1*, 3597 (1963).
18. T. L. Smith, in *Rheology*, F. R. Eirich, Ed., Academic Press, New York, 1969, Vol. 5, p. 127.
19. P. W. Ogden, *Non-linear Elastic Deformations*, Wiley, New York, 1984.
20. H. G. Killian and H. Schenk, *J. Appl. Polym. Sci.*, **35**, 345 (1988).
21. E. Kreyszig, *Advanced Engineering Mathematics*, Wiley, New York, 1983.
22. N. Warren, *J. Geophys. Res.*, **78**(2), 352 (1973).
23. A. Green and J. Adkins, *Large Elastic Deformations*, Clarendon Press, Oxford, 1970.

Received May 25, 1995

Accepted July 20, 1995